

Accepted Manuscript

Synthesis, antitumor evaluation and 3D-QSAR studies of [1,2,4]triazolo[4,3-b]
[1,2,4,5]tetrazine derivatives

Feng Xu, Zhen-zhen Yang, Zhong-lu Ke, Li-min Xi, Qi-dong Yan, Wei-qiang
Yang, Li-qing Zhu, Fei-lei Lin, Wei-ke Lv, Han-gui Wu, John Wang, Hai-bo Li

PII: S0960-894X(16)30909-X
DOI: <http://dx.doi.org/10.1016/j.bmcl.2016.08.078>
Reference: BMCL 24204

To appear in: *Bioorganic & Medicinal Chemistry Letters*

Received Date: 26 June 2016
Revised Date: 19 August 2016
Accepted Date: 24 August 2016



Please cite this article as: Xu, F., Yang, Z-z., Ke, Z-l., Xi, L-m., Yan, Q-d., Yang, W-q., Zhu, L-q., Lin, F-l., Lv, W-k., Wu, H-g., Wang, J., Li, H-b., Synthesis, antitumor evaluation and 3D-QSAR studies of [1,2,4]triazolo[4,3-b][1,2,4,5]tetrazine derivatives, *Bioorganic & Medicinal Chemistry Letters* (2016), doi: <http://dx.doi.org/10.1016/j.bmcl.2016.08.078>

This is a PDF file of an unedited manuscript that has been accepted for publication. As a service to our customers we are providing this early version of the manuscript. The manuscript will undergo copyediting, typesetting, and review of the resulting proof before it is published in its final form. Please note that during the production process errors may be discovered which could affect the content, and all legal disclaimers that apply to the journal pertain.



Synthesis, antitumor evaluation and 3D-QSAR studies of [1,2,4]triazolo[4,3-b][1,2,4,5]tetrazine derivatives

Feng Xu^{a,*}, Zhen-zhen Yang^a, Zhong-lu Ke^a, Li-min Xi^a, Qi-dong Yan^a, Wei-qiang Yang^b, Li-qing Zhu^a, Fei-lei Lin^a, and Wei-ke Lv^a, Han-gui Wu^a, John Wang^c and Hai-bo Li^d

^a Chemical Pharmaceutical Research Institute, Taizhou Vocational & Technical College, Taizhou 318000, PR China

^b, Zhe Jiang Hisoar Pharmaceutical CO.LTD. Taizhou 318000, PR China

^c ImmuOn Therapeutics, Chenqiao BridgePark, Nantong 226003, PR China

^d Department of Clinical Laboratory Medicine, Nantong Maternity and Child Health Hospital, Nantong 226018, PR China

ARTICLE INFO

Article history:

Received

Revised

Accepted

Available online

Keywords:

Triazole

Tetrazine

X-ray diffraction

Antiproliferative activity

3D-QSAR

CoMFA

CoMSIA

ABSTRACT

A series of [1,2,4]triazolo[4,3-*b*][1,2,4,5] tetrazine derivatives have been synthesized and their structures were confirmed by single-crystal X-ray diffraction. Compared to some reported structures of 1,6-dihydro-1,2,4,5-tetrazine, these compounds can't be considered as having homoaromaticity. Their antiproliferative activities were evaluated against MCF-7, Bewo and HL-60 cells in vitro. Two compounds were highly effective against MCF-7, Bewo and HL-60 cells with IC₅₀ values in 0.63-13.12 μM. Three-dimensional quantitative structure-activity relationship (3D-QSAR) studies of comparative molecular field analysis (CoMFA) and comparative molecular similarity indices analysis (CoMSIA) were carried out on 51 [1,2,4]triazolo[4,3-*b*][1,2,4,5] tetrazine derivatives with antiproliferative activity against MCF-7 cell. Models with good predictive abilities were generated with the cross validated q^2 values for CoMFA and CoMSIA being 0.716 and 0.723, respectively. Conventional r^2 values were 0.985 and 0.976, respectively. The results provide the tool for guiding the design and synthesis of novel and more potent tetrazine derivatives.

2009 Elsevier Ltd. All rights reserved.

* Corresponding author. Tel.: +86-576-88663357; fax: +86-576-88663352; E-mail: xufeng901@126.com.

1,2,4,5-Tetrazine derivatives have a high potential for biological activity, such as antimite activity,¹ herbicidal activity,² antimalarial activity,³ antiviral activity,⁴ antiinflammatory activity,⁵ antibacterial activity,⁶ and antitumor activity.⁷⁻¹⁰ There are four possible series of dihydro-1,2,4,5-tetrazines, the 1,2-, 1,4-, 1,6- and 3,6-dihydro-1,2,4,5-tetrazines, respectively. There are many reports on synthesis and biological activity of 1,4-dihydro- and 1,2-dihydro-1,2,4,5-tetrazine derivatives.¹¹⁻²⁰ However, there are only a few reports on the 1,6-dihydro-1,2,4,5-tetrazines and their derivatives.²¹⁻²⁷ Most of them were considered as showing homoaromaticity.

Quantitative structure–activity relationship (QSAR) modeling results in a quantitative correlation between chemical structure and properties (such as biological activity), it can be also applied to predict biological activity of nonsynthesized compounds structurally related to a training set of compounds. Among techniques of three-dimensional quantitative structure–activity relationship (3D-QSAR), comparative molecular field analysis (CoMFA) and comparative molecular similarity indices analysis (CoMSIA) are two powerful prevailing methodologies,^{28,29} which are the most widely used for the study of compounds with potential biological activity.

Recently, our group has reported a series of 6-substituted-[1,2,4]triazolo[4,3-b][1,2,4,5] tetrazines, which also can be considered to be belonged to 1,6-dihydro-1,2,4,5-tetrazine derivatives, and found them with potent antiproliferative activities against MCF-7, Bewo and HL-60 cells and c-Met kinase inhibitory activities.³⁰ In continuation of this work, we researched the synthesis, antitumor evaluation and 3D-QSAR studies of [1,2,4] triazolo[4,3-b][1,2,4,5] tetrazine compounds and attempted to investigate how the substituents located at the 3-positions of the [1,2,4]triazolo[4,3-b][1,2,4,5]tetrazine ring influence antitumour activity. In this letter, thirty five [1,2,4]triazolo[4,3-b][1,2,4,5] tetrazines were synthesized. The reactions employed for the synthesis of [1,2,4]triazolo[4,3-b][1,2,4,5]tetrazines are summarised in Scheme 1.³¹ The starting material **1** was prepared to accord to the published method.³² Compound **2** was prepared from the reaction of compound **1** and 80% hydrazine hydrate in acetonitrile at room temperature.³³ Subsequent schiff base reaction was conducted between **2** and aldehyde in ethanol to obtain corresponding schiff bases **3**,³⁴ which were then treated with lead tetraacetate in chloroform to yield 3-substituted-6-(3,5-dimethyl-1*H*-pyrazol-1-yl)-[1,2,4] triazolo[4,3-b][1,2,4,5] tetrazines **5**;³⁵ compounds **2** reacted with acyl chloride to yield corresponding acylhydrazines **4**,³² subsequent cyclization of **4** with phosphoryl chloride also obtained compounds **5**. Compounds **5** were then treated with different alkyl amines in ethyl acetate to obtain **6**. The results are summarized in Table 1.³⁶

To test the antitumor activities of the synthesized compounds, we evaluated antiproliferative activities of compounds **5** and **6** against MCF-7, Bewo and HL-60 cells by MTT assay. The results were summarized in Table 2. As illustrated in Table 2, the active analogs showed a remarkable cytotoxic activity. Particularly, it should be noticed that compounds **5l** (12.82 μ M for MCF-7, 6.70 for Bewo and 0.67 for HL-60 respectively) and **6f** (13.12 μ M for MCF-7, 4.09 for Bewo and 0.63 for HL-60 respectively) showed the most potent biological activity, comparable to the positive control cisplatin (15.33 μ M for MCF-7, 15.66 μ M for Bewo and 16.66 μ M for HL-60 cells respectively). Comparison with the reported compounds³⁰ (no substituents on C₃-position) and the compounds **5a-6v**, the antiproliferative activity against MCF-7 was decreased obviously when the substituents at C₃ position of

triazolotetrazine ring increased; on the contrary, the antiproliferative activity against Bewo and HL-60 was slightly increased when the substituents at C₃ position of triazolotetrazine ring increased, especially when C₃ position of triazolotetrazine ring tolerated some alkyl groups(**5g-k**). Comparing the compounds **6a-v**, it had the trends that when the substituents such as F, NO₂ and MeO on the *para*-position of benzene ring decreased the inhibitory activities (e.g. **6c**, **6g**, **6h**, **6i**, **6l** and **6m**); while the substituents such as Cl on the *ortho*- or *para*-position of benzene ring could increase the inhibitory activities (e.g. **6j**, **6k**, **6n** and **6o**); the compounds tolerated alkyl substituents at C₃ position of triazolotetrazine ring (**6p-v**) showed the moderate inhibitory activities between above both cases.

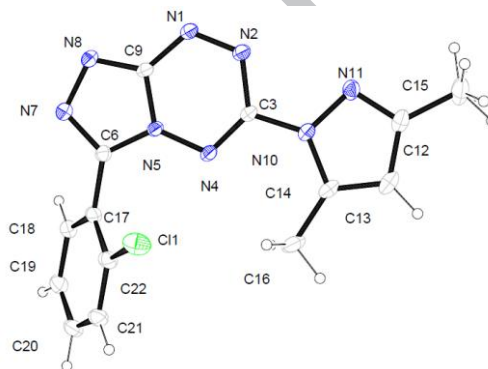
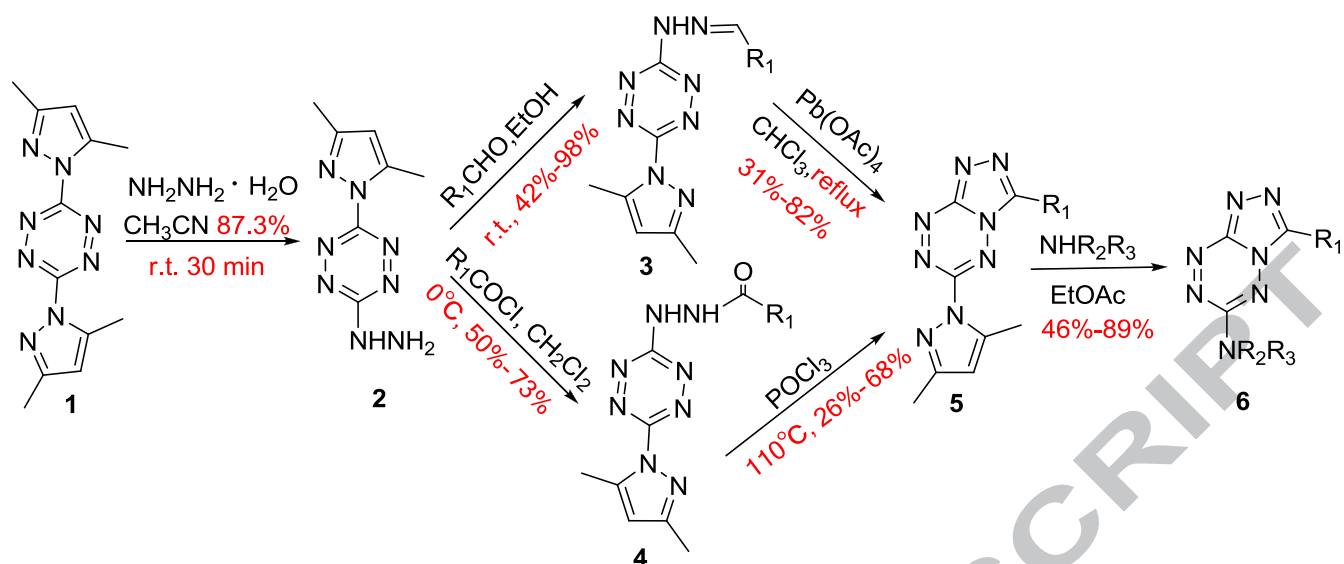


Figure 1. The X-ray crystal structure of compound **5c**, shown with 30% probability displacement ellipsoid.

Single-crystal structures of compound **5c** were determined by X-ray crystallography,³⁷⁻³⁹ and its molecular structure is illustrated in Figure 1. In the molecule of **5c**, the 1,2,4,5-tetrazine ring and 1,2,4-triazole ring are almost coplanar within 0.02 Å. The atoms N1 and N5 are both *sp*² hybridised, and their π orbitals are parallel to each other and can't overlap, which is different from the compounds 3-phenyl-6-methyl-1,6-dihydro-1,2,4,5-tetrazine²¹ and 3-phenyl-6-ethyl-1,6-dihydro-1,2,4,5-tetrazine²², so the molecule can't be considered as having homoaromaticity. The pyrazol ring and benzene ring make dihedral angles of 6.81 (2)° and 54.29 (3)°, respectively, with the bicyclic plane. The large dihedral angle between benzene ring and bicyclic plane was caused by the steric effect of chlorine atom on the *ortho*-position of benzene ring. From Table 2, it is obvious that compounds **5c**, **6j**, **6k** and **6o** that having *ortho*-substituents on benzene ring showed better antiproliferative activity against Bewo than the others that having *para*-substituents on benzene ring (**6c**, **6g-i**, **6l-m**), which indicated that the conformation of large dihedral angle between benzene ring and bicyclic plane may be beneficial to antiproliferative activity.



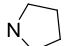

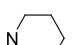
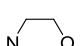
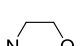
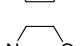
In addition, we combined the inhibition data of compounds **5** and **6** (Table 3) to those of our previously reported 6-substituted-[1,2,4]triazolo[4,3-b][1,2,4,5] tetrazines (**7-29**, Table 3),³⁰ and developed CoMFA and CoMSIA 3D-QSAR models.^{40,41} A total of 51 [1,2,4]triazolo[4,3-b][1,2,4,5] tetrazine derivatives, divided into training and test sets, were used for model building and validation, respectively.⁴²⁻⁴⁷ The statistical parameters for CoMFA and CoMSIA models were given in Table 4. The CoMFA model ($q^2 = 0.716$, $r^2 = 0.985$) was based on the steric and electrostatic fields, and the CoMSIA model ($q^2 = 0.723$, $r^2 = 0.976$) was based on the steric, electrostatic, hydrophobic, hydrogen bond donor and hydrogen bond acceptor fields. These models revealed a beneficial response to test set validation. Partial least-squares (PLS) analysis was performed

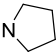
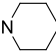
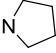
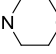
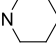
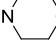
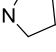
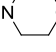
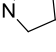
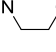
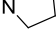
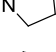
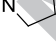

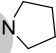
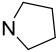


3a: phenyl; **3b:** 4-fluorophenyl; **3c:** 2,4-dichlorophenyl; **3d:** 4-nitrophenyl; **3e:** 4-methoxyphenyl; **3f:** 2-chlorophenyl; **3g:** Me; **3h:** benzyl
4a: 4-methylphenyl; **4b:** phenyl; **4c:** 4-chlorophenyl; **4d:** 4-nitrophenyl; **4e:** 2-nitrophenyl; **4f:** Me; **4g:** Et; **4h:** i-Pr; **4i:** t-Bu; **4j:** n-pentyl; **4k:** cyclohexyl; **4l:** benzyl

Scheme 1

Table 1. Structure of compounds 5 and 6.

Compound	R ¹	NR ¹ R ²	Mp(°C)	Yield(%)
5a	4-Methylphenyl	—	198-200	31 ^c , 26 ^d
5b^a	4-Methoxyphenyl	—	125-127	58 ^c
5c^a	2-Chlorophenyl	—	209-211	62 ^c
5d^a	Phenyl	—	151-153	41 ^c , 35 ^d
5e^a	4-Nitrophenyl	—	235-237	73 ^c , 56 ^d
5f	4-Chlorophenyl	—	217-220	75 ^c
5g	Me	—	176-179	65 ^c , 45 ^d
5h	Et	—	143-145	52 ^d
5i	CH(CH ₃) ₂	—	108-110	46 ^d
5j	C(CH ₃) ₃	—	180-183 ^b	66 ^d
5k	CH ₂ (CH ₂) ₃ CH ₃	—	99-101	46 ^d
5l		—	156-158	68 ^d
5m	Benzyl	—	128-130	82 ^c , 65 ^d
6a	Phenyl		185-188	75
6b	Phenyl		254-256	78
6c	4-Fluorophenyl		246-248 ^b	85
6d	4-Fluorophenyl		190-192	72
6e	4-Fluorophenyl		218-220 ^b	76
6f	4-Chlorophenyl		239-241	68
6g	4-Nitrophenyl		255-258 ^b	86

6h	4-Nitrophenyl		235-237 ^b	89
6i	4-Nitrophenyl		238-241 ^b	79
6j	2-Chlorophenyl		190-192 ^b	85
6k	2-Chlorophenyl		218-220	79
6l	4-Methoxyphenyl		260-262	52
6m	4-Methoxyphenyl		183-185	57
6n	2,4-Dichlorophenyl		169-170	78
6o	2,4-Dichlorophenyl		208-210	82
6p	Me		104-106	54
6q	Me		146-148	46
6r	Et		134-135	65
6s	CH(CH ₃) ₂		96-97	68
6t	C(CH ₃) ₃		144-146	81
6u			124-126	78
6v	CH ₂ (CH ₂) ₃ CH ₃		62-64	66

^a These compounds have been reported in literature³⁶.

^b Decomposition temperatures.

^c Based on compounds **3**.

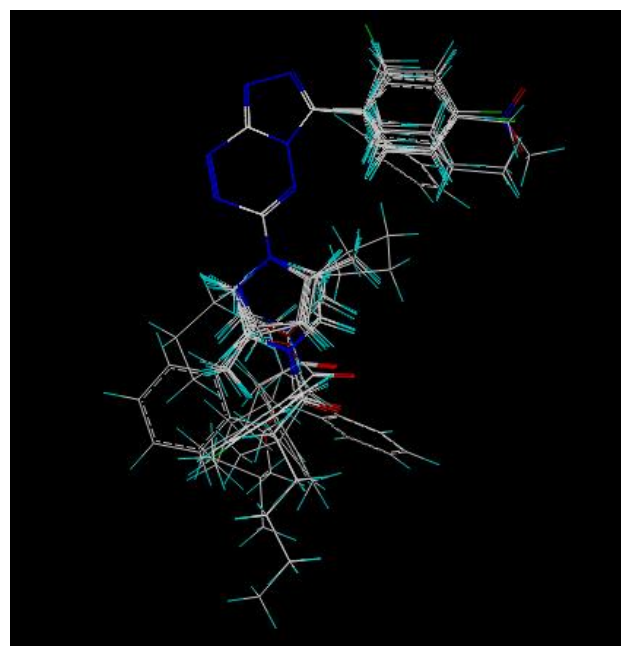
^d Based on compounds **4**.

Table 2. Antitumor activities against MCF-7, Bewo and HL-60 cell lines in vitro (IC_{50} in μM)

Compound	$IC_{50}(\mu M)$		
	MCF-7	Bewo	HL-60
5a	36.20	7.54	>100
5b ^a	16.72	18.30	>100
5c ^a	19.47	3.21	73.58
5d ^a	13.65	23.64	12.11
5e ^a	6.85	7.29	>100
5f	5.57	22.62	>100
5g	17.81	2.61	0.43
5h	36.03	1.64	0.82
5i	33.68	2.32	1.16
5j	17.63	0.73	0.73
5k	22.00	2.79	1.05
5l	12.82	6.70	0.67
5m	54.84	2.29	2.61
6a	8.87	5.65	30.36
6b ^b	>100	>100	>100
6c ^b	>100	>100	4.56
6d	41.43	3.34	30.74
6e	32.86	4.65	28.88
6f	13.12	4.09	0.63
6g	>100	>100	5.79
6h	>100	>100	>100
6i	>100	>100	0.61
6j	29.56	2.99	2.66
6k	14.93	3.15	13.25
6l	>100	>100	12.85
6m	>100	8.94	38.97
6n	19.59	8.06	8.65
6o	19.32	1.71	4.84
6p	44.83	5.36	29.72
6q	38.90	5.88	4.52
6r	47.01	5.02	47.01
6s	46.76	3.43	71.21
6t	55.02	12.54	>100
6u	37.70	21.96	23.79
6v	42.86	27.93	42.48
Cisplatin	15.33	15.66	16.66

^a These compounds have been reported in literature³⁶.^b These compounds were poor solubility in DMSO.

to establish a linear relationship between the molecular fields and the activity of molecules. Experimental and predicted pIC_{50} values for the training set and test set are reported in **Table 5**. **Figure 2** shows the alignment of all compounds used in the training set. Contour maps for the CoMFA and CoMSIA models are displayed in **Figure 3**. The relationship between actual and predicted pIC_{50} of the training set and test set compounds of CoMFA and CoMSIA models are illustrated in **Figures 4 and 5**.

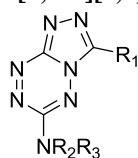
**Figure 2.** Alignment of all target compounds in the training set.

Steric CoMFA map (**Fig. 3A**) showed green contour around 6-position of triazolotetrazine ring indicating bulky groups were favored at this position. It was confirmed that the compounds **17**, **22-30** exhibited higher antiproliferative activity. The yellow contours around 3-position of triazolotetrazine ring indicated that compounds with bulky and non-coplanar groups at this position were less potent. This explained that the compounds **5a-5d**, **5g-5m** and **6a-6t** had not good antiproliferative activity.

Electrostatic CoMFA contour map (**Fig. 3B**) was shown in red around 6-position of triazolotetrazine ring indicating that negative charge might play a favorable role on activity. Compounds **19-29**, **6a**, **6f**, **6k** and **6o** showed higher activity owing to the existence of oxygen in the carbonyl group or in the morpholine ring. The blue contours surrounding the 2- and 4-positions of benzene ring on 3-position of triazolotetrazine ring showed that electronegative atom was disfavored at these positions. The compounds **5a-c** and **6d-j** were good examples.

The colors of the steric and electrostatic contour maps in the CoMSIA model (**Fig. 3C and 3D**) have the same meanings as those of the CoMFA model. In agreement with CoMFA, yellow contours and green contours are observed at the same position. Similar to CoMFA, red contours and blue contours are observed at the almost same position. Unlike CoMFA, the yellow contour is bigger at the 3-position and also observed at 6-positions, the blue contour is disappeared at 4-position of benzene ring and also observed at 6-position of triazolotetrazine ring.

Hydrophobic contour maps (**Fig. 3E**) show gray around 3- and 6-positions on triazolotetrazine nucleus indicating that hydrophobic groups are disfavored at these positions. The contour can be explained by the presence of the substituted phenyl and alkyl at 3-position, which in most cases produces less active compounds. This contour is in agreement with the yellow contour at the same position in CoMFA and CoMSIA steric contour maps (**Fig. 3A and 3C**). Two favorable yellow regions are observed at 3- and 6-positions, which indicated that hydrophobic groups are favored at these positions. The former contour explained that the compounds (**6k-6o**) having chlorine atom on the 2-position of benzene ring are more potent. The latter contour is in agreement with the green contour at the same

Table 3. Chemical structures of [1,2,4]triazolo[4,3-b][1,2,4,5]tetrazine derivatives used in this study

Comd	R ₁	NR ₁ R ₂	Comd	R ₁	NR ₁ R ₂
5a	4-Methylphenyl	3,5-Dimethyl-1 <i>H</i> -pyrazol-1-yl	6u	Cyclohexyl	Pyrrolid-1-yl
5b	4-Methoxyphenyl	3,5-Dimethyl-1 <i>H</i> -pyrazol-1-yl	6v	CH ₂ (CH ₂) ₃ CH ₃	Pyrrolid-1-yl
5c	2-Chlorophenyl	3,5-Dimethyl-1 <i>H</i> -pyrazol-1-yl	7	H	NH ₂
5d	Phenyl	3,5-Dimethyl-1 <i>H</i> -pyrazol-1-yl	8	H	NH(CH ₂) ₂ CH ₃
5e	4-Nitrophenyl	3,5-Dimethyl-1 <i>H</i> -pyrazol-1-yl	9	H	NH(CH ₂) ₃ CH ₃
5f	4-Chlorophenyl	3,5-Dimethyl-1 <i>H</i> -pyrazol-1-yl	10	H	NH(CH ₂) ₂ OH
5g	Me	3,5-Dimethyl-1 <i>H</i> -pyrazol-1-yl	11	H	NH- cyclopentane
5h	Et	3,5-Dimethyl-1 <i>H</i> -pyrazol-1-yl	12	H	NH-cyclohexane
5i	CH(CH ₃) ₂	3,5-Dimethyl-1 <i>H</i> -pyrazol-1-yl	13	H	Piperid-1-yl
5j	C(CH ₃) ₃	3,5-Dimethyl-1 <i>H</i> -pyrazol-1-yl	14	H	NHCH ₂ CH ₂ -phenyl
5k	CH ₂ (CH ₂) ₃ CH ₃	3,5-Dimethyl-1 <i>H</i> -pyrazol-1-yl	15	H	4-CH ₃ -piperazin-1-yl
5l	Cyclohexyl	3,5-Dimethyl-1 <i>H</i> -pyrazol-1-yl	16	H	4-Benzyl-piperazin-1-yl
5m	Benzyl	3,5-Dimethyl-1 <i>H</i> -pyrazol-1-yl	17	H	4-COCH ₃ -piperazin-1-yl
6a	Phenyl	Morpholin-4-yl	18	H	4-COCH ₂ CH ₃ -piperazin-1-yl
6d	4-Fluorophenyl	Piperid-1-yl	19	H	4-CO(CH ₂) ₂ CH ₃ -piperazin-1-yl
6e	4-Fluorophenyl	Morpholin-4-yl	20	H	4-CO(CH ₃) ₃ CH ₃ -piperazin-1-yl
6f	4-Chlorophenyl	Morpholin-4-yl	21	H	4-CO(CH ₃) ₄ CH ₃ -piperazin-1-yl
6j	2-Chlorophenyl	Pyrrolid-1-yl	22	H	4-COC(CH ₃) ₃ -piperazin-1-yl
6k	2-Chlorophenyl	Morpholin-4-yl	23	H	4-COOCH ₂ CH(CH ₃) ₂ -piperazin-1-yl
6n	2,4-Dichlorophenyl	Pyrrolid-1-yl	24	H	4-(CO-benzyl)-piperazin-1-yl
6o	2,4-Dichlorophenyl	Morpholin-4-yl	25	H	4-(CO- cyclohexane) -piperazin-1-yl
6p	Me	Pyrrolid-1-yl	26	H	4-(CO-phenyl)-piperazin-1-yl
6q	Me	Morpholin-4-yl	27	H	4-(CO-(4-chlorophenyl))-piperazin-1-yl
6r	Et	Pyrrolid-1-yl	28	H	4-(CO-(4-methylphenyl))-piperazin-1-yl
6s	CH(CH ₃) ₂	Pyrrolid-1-yl	29	H	4-(CO-(4-nitrophenyl))-piperazin-1-yl
6t	C(CH ₃) ₃	Pyrrolid-1-yl			

Table 4. Summary of statistical data and validation for CoMFA and CoMSIA models

PLS statistics	CoMFA	CoMSIA
q^2 ^a	0.716	0.723
r^2 ^b	0.985	0.976
s^c	0.061	0.079
F ^d	239.517	127.396
ONC ^e	9	10
Steric ^f	0.668	0.317
Electrostatic ^g	0.332	0.222
Donor ^h		0.139
Acceptor ^h		0.058
Hydrophobic ⁱ		0.263

^a Cross-validated correlation coefficient from leave-one-out.^b Noncross-validated r^2 .^c Standard error of estimate.^d F-test value.^e Optimum number of principal components.^f Steric field contribution.^g Electrostatic field contribution.^h Donor and acceptor, of hydrogen bond fields contribution, respectively.ⁱ Hydrophobic field contribution.

position in CoMFA and CoMSIA steric contour maps (**Fig. 3A** and **3C**).

Donor and acceptor CoMSIA contour maps (**Fig. 3F**) showed that one big red contour around 4-position of pyrazole ring (for compounds **5a-5m**) or carbonyl group (for compounds **17-29**) at 6-position of triazolotetrazine nucleus suggested that hydrogen bond donor was disfavored at this area. This can explain that the

Table 5 Experimental and predicted pIC₅₀ values of compounds

Compd	Actual IC ₅₀ (μM)	Actual pIC ₅₀ ^b	CoMFA		CoMSIA	
			Predicted pIC ₅₀ ^b	Residual	Predicted pIC ₅₀ ^b	Residual
5a	36.20	4.441	4.432	0.009	4.515	-0.074
5b	16.72	4.777	4.796	-0.019	4.781	-0.004
5c	19.47	4.711	4.871	-0.160	4.773	-0.062
5d	13.65	4.865	4.836	0.029	4.788	0.077
5e	6.85	5.164	5.062	0.102	5.178	-0.014
5f ^a	5.57	5.254	5.041	0.213	5.025	0.229
5g	17.81	4.749	4.607	0.142	4.595	0.154
5h	36.03	4.443	4.540	-0.097	4.539	-0.096
5i	33.68	4.473	4.522	-0.049	4.526	-0.053
5j	17.63	4.754	4.676	0.078	4.687	0.067
5k	22.00	4.658	4.643	0.015	4.645	0.013
5l ^a	12.82	4.892	5.054	-0.162	4.949	-0.057
5m	54.84	4.261	4.218	0.043	4.279	-0.018
6a ^a	8.87	5.052	5.061	-0.009	4.780	0.272
6d	41.43	4.383	4.406	-0.023	4.378	0.005
6e	32.86	4.483	4.518	-0.035	4.479	0.004
6f ^a	13.12	4.882	5.070	-0.188	4.800	0.082
6j	29.56	4.529	4.554	-0.025	4.585	-0.056
6k ^a	14.93	4.826	4.984	-0.158	4.699	0.127
6n ^a	19.59	4.708	5.045	-0.337	4.781	-0.073
6o	19.32	4.714	4.712	0.002	4.652	0.062
6p	44.83	4.348	4.361	-0.013	4.397	-0.049
6q	38.90	4.410	4.461	-0.051	4.471	-0.061
6r	47.01	4.328	4.375	-0.047	4.297	0.031
6s	46.76	4.330	4.266	0.064	4.227	0.103
6t	55.02	4.260	4.339	-0.079	4.369	-0.109
6u	37.70	4.424	4.351	0.073	4.370	0.054
6v	42.86	4.368	4.394	-0.026	4.343	0.025
7	46.46	4.333	4.323	0.01	4.325	0.008
8 ^a	19.81	4.703	4.719	-0.016	4.768	-0.065
9	13.66	4.864	4.827	0.037	4.779	0.085
10	11.59	4.936	4.887	0.049	5.012	-0.076
11	88.20	4.055	4.034	0.021	4.065	-0.01
12	3.51	5.454	5.442	0.012	5.418	0.036
13	27.19	4.566	4.567	-0.001	4.559	0.007
14	1.24	5.905	5.942	-0.037	5.928	-0.023
15	21.57	4.666	4.681	-0.015	4.653	0.013
16	27.27	4.564	4.612	-0.048	4.593	-0.029
17	13.86	4.858	4.812	0.046	4.819	0.039
18	14.83	4.829	4.837	-0.008	4.973	-0.144
19	6.91	5.160	5.180	-0.02	5.218	-0.058
20	2.76	5.560	5.583	-0.023	5.424	0.136
21 ^a	5.26	5.279	5.639	-0.360	5.165	0.114
22	5.51	5.259	5.236	0.023	5.323	-0.064
23	5.39	5.269	5.268	0.001	5.233	0.036

24	3.08	5.511	5.474	0.037	5.509	0.002
25	1.26	5.898	5.910	-0.012	5.914	-0.016
26	8.38	5.077	5.043	0.034	4.928	0.149
27	12.85	4.891	4.882	0.009	4.896	-0.005
28	15.88	4.799	4.846	-0.047	4.883	-0.084
29 ^a	4.53	5.344	5.425	-0.081	5.164	0.180

^a Compounds in the tests set.

^b $pIC_{50} = -\log(IC_{50})$

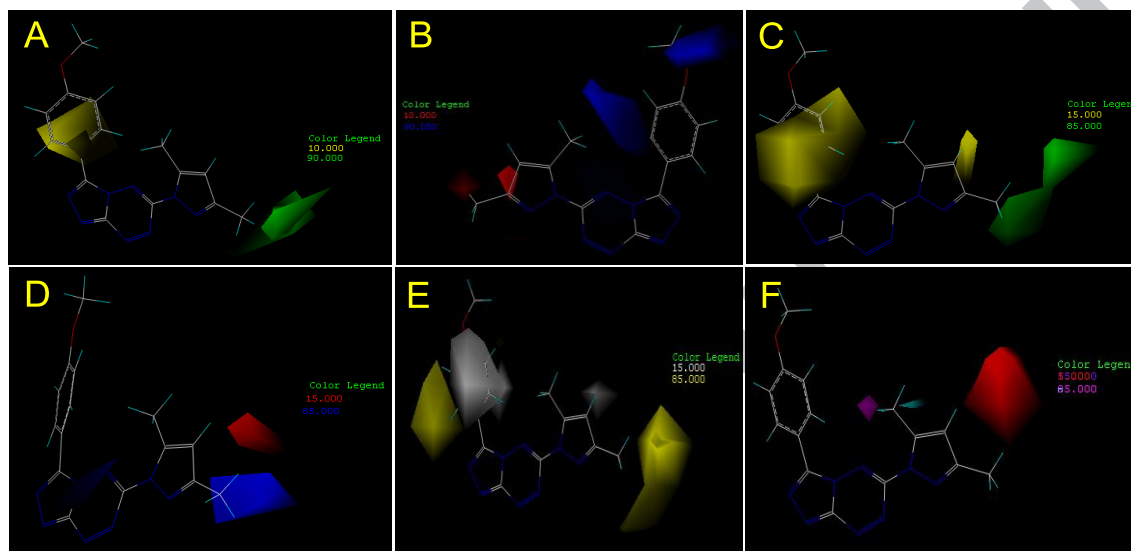


Figure 3. CoMFA and CoMSIA STDEV/COEFF contour maps. CoMFA model: (A) Sterically favored areas are in green, and sterically disfavored areas are in yellow. (B) Negative charge favored areas are in red and disfavored areas are in blue. CoMSIA model: The colors in (C) and (D) have the same meanings as do CoMFA contour maps (A) and (B), respectively. (E) Hydrophobic favored areas are in yellow and disfavored areas are in gray. (F) Donor and acceptor favored areas are in cyan and magenta, respectively, and donor and acceptor disfavored areas are in purple and red, respectively.

compounds **6e**, **6k**, **6o** and **6q** containing morpholine ring showed better antiproliferative activity than **6d**, **6j**, **6n** and **6p**, respectively. Cyan contour was observed around the 5-position of pyrazole ring (for compounds **5a-5m**) or 2-position of piperazine ring (for compounds **17-29**) at 6-position of triazolotetrazine nucleus suggested that hydrogen bond donor favored at this position. One small magenta contour was observed around benzene ring at 3-position of triazolotetrazine ring suggested that hydrogen bond acceptor were favored at this position. This gives us a hint that introduction hydrogen bond acceptors (e.g. C=O, NO₂) on the 2- or 3- positions of benzene ring may increase the antiproliferative activity.

The analysis of contour maps for CoMFA and CoMSIA models indicates that larger groups at 3-position with hydrophobic segments generate less active compounds. Substitutions at 3-position with hydrogen atom are favored over other substitutions in the current data set. Also, larger groups at 6-position with negative charges that could act as hydrogen bond acceptors could play favorable roles in activity.

In conclusion, [1,2,4]triazolo[4,3-b][1,2,4,5] tetrazine derivatives were synthesized. They were confirmed by single-crystal X-ray diffraction and evaluated against MCF-7, Bewo and HL-60 cells in vitro. The results of their antitumor activities show several compounds to be endowed with cytotoxicity in the low micromolar range and there are two compounds of **5l** and **6f**, which are highly effective against all tested cell lines with IC₅₀ in 0.63-13.12 μ M. The CoMFA and CoMSIA 3D-QSAR models were generated, showed good q^2 and r^2 values, and revealed a

beneficial response to test set validation. These models provide the tool for guiding the design and synthesis of novel and more potent tetrazine derivatives.

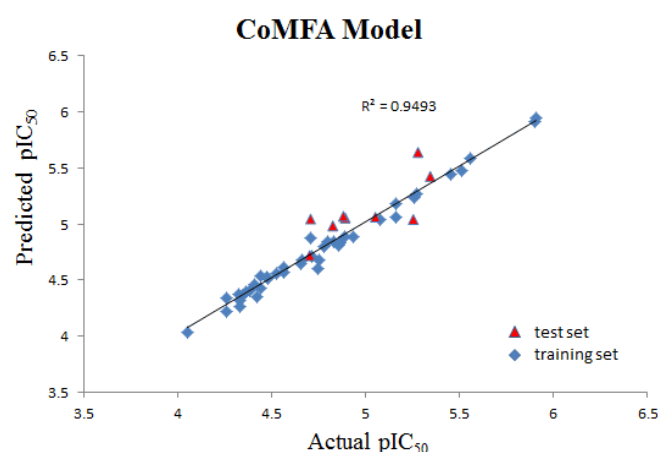


Figure 4. Plot of actual predicted activities for training set and test set based on CoMFA model.

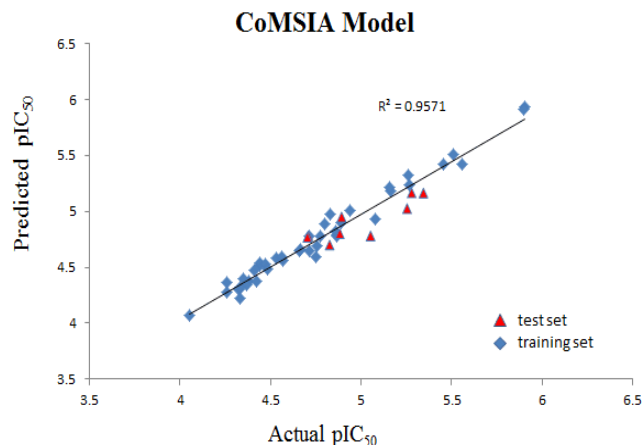


Figure 5. Plot of actual predicted activities for training set and test set based on CoMSIA model.

Acknowledgments

The authors are very grateful to the Marine Biological Resources Exploitation and Utilisation of Science and Technology Innovation Team of Taizhou (Document of CPC Taizhou Municipal Committee Office of Zhejiang Province NO.(2012) 58), the Scientific Project of Taizhou Vocational & Technical College (2016ZJ08) and The Taizhou "211" Talent Project Funding Scheme.

References and notes

- Falfushynska, H. I.; Gnatyshyna, L. L.; Stoliar, O. B. *Comp. Biochem. Physiol., Part C: Toxicol. Pharmacol.* **2012**, *155*, 396.
- Zhu, Y.-Q.; Cheng, J.; Zou, X.-M.; Hu, F.-Z.; Xiao, Y.-H.; Yang, H.-Z. *Chin. J. Org. Chem.* **2008**, *28*, 1044.
- Nhu, D.; Duffy, S.; Avery, V. M.; Hughes, A.; Baell, J. B. *Bioorg. Med. Chem. Lett.* **2010**, *20*, 4496.
- Pandey, V. K. *Indian Drugs* **1986**, *23*, 500.
- Sharma, P.; Kumar, A.; Sahu, V.; Singh, J. *Arkivoc (Gainesville, FL, US)* **2008**, 218.
- Tabassum, S.; Parveen, M.; Ali, A.; Alam, M.; Ahmad, A.; Khan, A. U.; Khan, R. A. *J. Mol. Struct.* **2012**, *1020*, 33.
- Sauer, J. In *Comprehensive Heterocyclic Chemistry II*; Katritzky, A. R., Rees, C. W., Scriven, E. F. V., Eds.; Pergamon: Oxford, 1996; Vol. 6, p 901.
- Stanovnik, B.; Grošelj, U.; Svete, J. In *Comprehensive Heterocyclic Chemistry III*; Katritzky, A. R., Ramsden, C. A., Scriven, E. F. V., Taylor, R. J. K., Eds.; Elsevier, 2008; Vol. 9, p 641.
- Neunhoeffer, H. In *Comprehensive Heterocyclic Chemistry*; Katritzky, A. R., Rees, C. W., Eds.; Pergamon: Frankfurt, 1984; Vol. 3, p 531.
- Eremeev, A. V.; Tikhomirov, D. A.; Tyusheva, V. A.; Liepins, E. *Khim. Geterosikl* **1978**, 753.
- Rao, G.-W.; Guo, Y.-M.; Hu, W.-X. *ChemMedChem* **2012**, *7*, 973.
- Rao, G.-W.; Wang, C.; Wang, J.; Zhao, Z.G.; Hu, W.-X. *Bioorg. Med. Chem. Lett.* **2013**, *23*, 6474.
- Rao, G.-W.; Hu, W.-X. *Bioorg. Med. Chem. Lett.* **2006**, *16*, 3702.
- Rao, G.-W.; Hu, W.-X. *Bioorg. Med. Chem. Lett.* **2005**, *15*, 3174.
- Sun, Y.Q.; Yuan, Q. *Synth. Commun.* **2003**, *16*, 2769.
- Yang, Z.-Z.; Xu, F.; Ke, Z.-L.; Chen, H.Y.; Hu, W.-X.; Li, H.-B. *J. Chem. Res.* **2013**, *37*, 586.
- Bansal, R. K.; Sharma, S. K. *J. Organomet. Chem.* **1978**, *155*, 293.
- Cohen, V.I. *J. Heterocyclic Chem.* **1978**, *15*, 1113.
- Foti, F.; Grassi, G.; Liotta, C.; Risitano, F. *Synlett* **2007**, *11*, 1730.
- Ito, S.; Kakehi, A.; Tanaka, Y.; Yoshida, K.; Matsuno, T. *B. Chem. Soc. Jpn.* **1979**, *52*, 483.
- Counotte-Potman, A.; van der Plas, H.C.; van Veldhuizen, B. *J. Org. Chem.* **1981**, *46*, 2138.
- Stam, C.H.; Counotte-Potman, A.D.; van der Plas, H.C. *J. Org. Chem.* **1982**, *47*, 2856.
- Jennison, C.P.R.; Mackay, D.; Watson, K.N.; Taylor, N. J. *J. Org. Chem.* **1986**, *51*, 3043.
- Xu, F.; Hu, W.-X. *J. Chem. Res.* **2008**, 212.
- Hu, W.-X.; Xu, F. *J. Chem. Res.* **2006**, 797.
- Xu, F.; Yang, Z.-Z.; Hu, W.-X.; Xi, L.-M. *Chin. J. Org. Chem.* **2010**, *2*, 260.
- Xu, F.; Yang, Z.-Z.; Zhang, S.-J.; Hu, W.-X. *Synthetic Commun.* **2011**, *41*, 3367.
- Sharma, H.; Cheng, X.; Buolamwini, J. K. *J. Chem. Inf. Model.* **2012**, *52*, 515.
- Sivan, S. K.; Manga, V. *J. Mol. Model.* **2012**, *18*, 569.
- Xu, F.; Yang, Z.-Z.; Jiang, J.-R.; Pan, W.-G.; Yang, X.-L.; Wu, J.-Y.; Zhu, Y.; Wang, J.; Shou, Q.-Y.; Wu, H.-G. *Bioorg. Med. Chem. Lett.* **2016**, *26*, 3042.
- Synthesis of compound **2**³³: To a mixture of **1** (20.5g, 76 mmol) in acetonitrile (228 ml) was added 80% hydrazine hydrate (4.7g, 76mmol) dropwise at 0 °C. A red precipitate formed immediately. The mixture was allowed to stir for 30 min at ambient temperature, filtered, washed with toluene and dried to give 10.2 g of pure material. The mother liquid was concentrated under reduced pressure and the residue treated with toluene, filtered and dried to give an additional 3.3 g of pure material for a combined yield of 87.3% of a red solid. m.p. 135-137 °C; IR ν_{\max} (KBr)/cm⁻¹: 3336, 3225, 2929, 1652, 1568, 1481, 1165, 1074; ¹H NMR (400MHz, DMSO-*d*₆) δ : 9.75(s, 1H, NH), 6.17(s, 1H, CH), 4.60(s, 2H, NH₂), 2.37(s, 3H, CH₃), 2.21(s, 3H, CH₃); ¹³CNMR(100MHz, DMSO-*d*₆) δ : 162.9, 157.0, 149.9, 141.2, 108.3, 13.2, 12.0. Synthesis of compound **5d** (Method A): The mixture of 3-(2-benzylidene hydrazinyl)-6-(3,5-dimethyl-1H-pyrazol-1-yl)-1,2,4,5-tetra- zine (**3a**, 10 mmol) and chloroform (20 ml) was heated to reflux. Lead tetraacetate (5.0 g, 11.4 mmol) in chloroform (10 ml) was added and the color of the solution was changed from wine red to yellow. After the starting **3a** was completely consumed (the reaction courses was monitored by TLC), evaporation of the chloroform, the crude yellow compound **5d** was obtained and purified by preparative thin-layer chromatography over silica gel PF 254 (2 mm, ethyl acetate). Yield: 41 %. mp 151-153 °C; ¹H NMR (400 MHz, CDCl₃): 8.56 (m, 2H), 7.63 (m, 3H), 6.26(s, 1H), 2.78(s, 3H), 2.42(s, 3H). EI-MS: *m/z* (%): 293.2[(M+H)⁺, 100]. Compounds of **5a-g** and **5m** were synthesized in the same manner. Synthesis of compound **5d** (Method B): The mixture of N'-(6-(3,5-dimethyl-1H-pyrazol-1-yl)-1,2,4,5-tetrazin-3-yl) benzohydrazide (**4b**, 10 mmol) and phosphoryl chloride (20 ml) was heated to 110 °C for 1 h. Then the mixture was cooled to 0 °C and poured into ice water (100ml). A solution of 10% sodium hydroxide was then added dropwise till pH = 7, resulting in the formation of a yellow solid product. The solid was filtered and washed thoroughly with water to yield the crude product that was recrystallized from 95% ethanol to give a pure product. Compounds of **5a**, **5d-e** and **5g-m** were synthesized in the same manner. Synthesis of compound **6a**: The mixture of compound **5d** (1.3 g, 4.6 mmol) and ethyl acetate (30 ml) was added to morpholine (0.4 g, 4.6 mmol). The mixture was stirred at room temperature for 30min, then warmed up to 60 °C. After the starting **5d** was completely consumed (the reaction courses was monitored by TLC), evaporation of ethyl acetate, the crude yellow compound **6a** was obtained and purified by preparative thin-layer chromatography over silica gel PF 254 (2 mm, ethyl acetate: petroleum ether = 1 : 1). Yield: 75 %. mp 185-188 °C; ¹H NMR (400 MHz, CDCl₃): 8.43-8.45 (m, 2H), 7.60-7.67 (m, 3H), 3.92 (s, 4H), 3.83 (m, 4H). IR ν_{\max} (KBr)/cm⁻¹: 2955, 1560, 1438, 1123, 1037, 702. ESI-MS: *m/z* (%): 284.3 [(M+H)⁺, 100]. Anal. calcd (%) for C₁₃H₁₃N₇O: C, 55.12; H, 4.63; N, 34.61; O, 5.65. Found: C, 55.17; H, 4.62; N, 34.55; O, 5.64. Compounds of **6b-v** were synthesized in the same manner. Data for other compounds are provided in the Supplementary data.
- Yan, Q. D.; Xu, J.; Chen, J. J. *Chin. J. Syn. Chem.* **2011**, *19*, 709.
- Chavez, D. E.; Hiskey, M. A. *J. Heterocyclic Chem.* **1998**, *35*, 1329.
- Chen, J.J.; Xu, F.; Yang, Z.Z. *Huaxue Tongbao* **2012**, *75*, 268.
- Rusinov, G. L.; Ganebnykh, I. N.; Chupakhin, O. N. *Russ. J. Org. Chem.* **1999**, *35*, 1350.
- Chen, H.; Zheng, C.X.; Yang, Y.F.; Lin, T.T.; Yuan, D.; Xu, F. *Chin. J. Syn. Chem.* **2012**, *20*, 475.
- Crystal data of compound **5c**: the crystal was obtained by slow evaporation from 95% ethanol at room temperature. A yellow prism of dimensions 0.40×0.38×0.31 mm³ was used for data collection on a Rigaku AFC10 diffractometer with a Saturn724+ CCD detector using graphite-monochromated MoK α radiation from a rotating anode graphite source (λ = 0.71073 Å) using the CrystalClear program.³⁸ The structures were solved with SHELXS97 and refined with the full-matrix least-squares procedure on F² by SHELXL97³⁹. All non-hydrogen atoms were located in a difference Fourier map and refined

anisotropically. All hydrogen atoms located at geometrically calculated positions and treated by a mixture of independent and constrained refinement. Other details of the structures have been deposited with the Cambridge Crystallographic Data Centre as deposition number CCDC 935921. $C_{14}H_{11}ClN_8$, Mr = 326.76, Monoclinic, $a = 8.115(2)$, $b = 20.605(6)$, $c = 9.136(3)$ Å, $\beta = 104.502(4)^\circ$, $U = 1479(2)$ Å³, $T = 153(2)$ K, space group: $P2_1/n$, $Z = 4$, $D_x = 1.468$ g cm⁻³, μ (MoK α) = 0.10 mm⁻¹, 12994 reflections measured, 3954 unique ($R_{int} = 0.032$) which were used in all calculations. Fine $R_I = 0.048$, $wR(F^2) = 0.115$ (all data).

38. Rigaku/MSD, CrystalClear. Rigaku/MSD Inc.; The Woodlands, Texas, **2008**.
39. Sheldrick, G.M. *Acta. Crystallogr.* **2008**, *A64*, 112.
40. CoMFA studies were performed with SYBYL-X 2.0 molecular modeling software.⁴¹ Steric and electrostatic interactions were calculated using a sp³ carbon probe atom with a charge of +1 with a distance-dependent dielectric at each lattice point, and energy cut-off of 30 kcal mol⁻¹. Each molecule was calculated on a 3D cubic lattice with grid spacing of 2 Å in x, y, and z directions. The CoMFA-STD method in SYBYL was used to scale CoMFA fields. Similarity indices were derived from the same lattice box, which were utilized in CoMFA calculations. Steric, electrostatic, hydrophobic, hydrogen bond donor and hydrogen bond acceptor descriptors were evaluated using the probe atom. GAUSSIAN-type distance dependence was used to measure the relative attenuation of the field position of each atom in the lattice and a default value of 0.3 was used as the attenuation factor.
41. SYBYL-X 2.0, Tripos Inc.: St. Louis, MO, 2012.
42. The IC₅₀ (concentration causing 50% inhibitory effect on the A549 proliferation) values were converted to pIC₅₀ (-log IC₅₀) values and used as dependent variables in the CoMFA and CoMSIA QSAR analysis. For 3D-QSAR analyses, 42 compounds (82.4%) were selected as the training set for model construction, and the remaining 9 compounds (17.6%) as the test set for model validation. The activities of the training set range from 1.24 μM (pIC₅₀ = 5.905) to 85.20 μM (pIC₅₀ = 4.055). The activities of the test set range from 4.53 μM (pIC₅₀ = 5.344) to 19.81 μM (pIC₅₀ = 4.703). The fact worth mentioning is that the structural diversity and activity range of the test set are comparable with the training set.⁴³⁻⁴⁵ In the development of 3D-QSAR models, the molecular alignment and conformation selection are the most essential steps. Conformations of each compound were generated using Confort™ conformation analysis. Energy minimizations were performed using Tripos force field⁴⁶ with a distance-dependent dielectric and Powell conjugate gradient algorithm with a convergence criterion of 0.005 kcal/(mol Å). Gasteiger-Hückel⁴⁷ charges were assigned to all molecules. Since specific molecular target is unknown to these compounds, the most active compound **14** was used as a template for superimposition, assuming that its conformation represents the most bioactive conformation of the tetrazine derivatives. All compounds were aligned using a tetrazine nucleus as common substructure in all molecules and minimum scaffold required for active molecules. **Figure 2** shows the alignment of all compounds in the training set.
43. Golbraikh, A.; Shen, M.; Xiao, Z. Y.; Xiao, Y. D.; Lee, K. H.; Tropsha, A. *J. Comput. Aided Mol. Des.* **2003**, *17*, 241.
44. Golbraikh, A.; Tropsha, A. *J. Mol. Graph. Model.* **2002**, *20*, 269.
45. Golbraikh, A.; Tropsha, A. *J. Comput. Aided Mol. Des.* **2002**, *16*, 357.
46. Clark, M.; Cramer, R. D., III; Van, O. N. *J. Comput. Chem.* **1989**, *10*, 982.
47. Gasteiger, J.; Marsili, M. *Tetrahedron* **1980**, *36*, 3219.

Supplementary Material

Supplementary data associated with this article can be found, in the online version, at <http://dx.doi.org/10.1016/j.bmcl.2013.0>

Click here to remove instruction text...

Graphical Abstract

A series of [1,2,4]triazolo[4,3-*b*][1,2,4,5] tetrazine derivatives have been synthesized and their antiproliferative activities were evaluated against MCF-7, Bewo and HL-60 cells in vitro. Two compounds were highly effective against MCF-7, Bewo and HL-60 cells with IC₅₀ values in 0.63-13.12 μ M. Three-dimensional quantitative structure–activity relationship (3D-QSAR) studies of comparative molecular field analysis (CoMFA) and comparative molecular similarity indices analysis (CoMSIA) were carried out on 51 [1,2,4]triazolo[4,3-*b*][1,2,4,5] tetrazine derivatives with antiproliferative activity against MCF-7 cell. Models with good predictive abilities were generated with the cross validated q^2 values for CoMFA and CoMSIA being 0.716 and 0.723, respectively. Conventional r^2 values were 0.985 and 0.976, respectively. The results provide the tool for guiding the design and synthesis of novel and more potent tetrazine derivatives.

Synthesis, antitumor evaluation and 3D-QSAR studies of [1,2,4]triazolo[4,3-*b*][1,2,4,5]tetrazine derivatives

Feng Xu^{a,*}, Zhen-zhen Yang^a, Zhong-lu Ke^a, Li-min Xi^a, Qi-dong Yan^a, Wei-qiang Yang^b, Li-qing Zhu^a, Fei-lei Lin^a, and Wei-ke Lv^a, Han-gui Wu^a, John Wang^c and Hai-bo Li^c

